**Inhibition of Src impairs the growth of met-addicted gastric tumors.**

UNIVERSITÀ DEGLI STUDI DI TORINO

# Inhibition of Src Impairs the Growth of Met-Addicted Gastric Tumors

Andrea Bertotti[1], Cecilia Bracco[1], Flavia Girolami[1], Davide Torti[1],Stefania Gastaldi[1], Francesco Galimi[1], Enzo Medico[2], Paul Elvin[3],Paolo M. Comoglio[1], and Livio Trusolino[1]

**Author Affiliations**

[1]Division of Molecular Oncology and [2]Laboratory of Functional Genomics, The Oncogenomics Center, Institute for Cancer Research and Treatment (IRCC), University of Torino Medical School, Candiolo, Turin, Italy and [3]Cancer and Infection Research Area, AstraZeneca, Macclesfield, Cheshire, United Kingdom

**Author Notes**

Current address for F. Girolami: Department of Animal Pathology, Division of Pharmacology and Toxicology, Faculty of Veterinary Medicine, University of Torino, 10095 Grugliasco, Turin, Italy.

**Corresponding Authors**:

Livio Trusolino or Paolo M. Comoglio, Division of Molecular Oncology, IRCC, Institute for Cancer Research and Treatment, University of Torino Medical School, Strada Provinciale 142, Km. 3.95, 10060 Candiolo, Turin, Italy. Phone: 39-11-993-3202; Fax: 39-11-993-3225; E-mail: livio.trusolino@ircc.it or paolo.comoglio@ircc.it.

A. Bertotti and C. Bracco contributed equally to this work.

## ABSTRACT

**Purpose**: We examined whether inhibition of Src tyrosine kinase, a downstream effector of the *MET* oncogene, can hinder the malignant properties of gastric tumors dependent on Met for growth and survival.

**Experimental Design**: Sensitivity to Src inhibition was determined *in vitro* by measuring clonogenic survival (anchorage-independent growth) and *in vivo* by establishing xenograft models. Four “Met-addicted” gastric carcinoma cell lines (GTL16, MKN45, HS746T, and SNU5) and three Met-independent gastric carcinoma cell lines (KATO III, AGS, and NCI-N87) were treated with the Src inhibitor saracatinib (AZD0530). In GTL16 and KATO III, Src neutralization was also achieved by dasatinib and RNA interference. The biochemical and transcriptional consequences of Src inhibition were explored using anti-phosphoprotein antibodies and oligonucleotide microarrays.

**Results**: Inhibition of Src in Met-addicted gastric carcinoma cell lines (*a*) decreased the phosphorylation/activation levels of signaling intermediates involved in cell proliferation and protection from apoptosis and down-modulated the expression of several cell cycle regulators; (*b*) reduced anchorage-independent growth; (*c*) enhanced impairment of cell viability produced by Met inhibition; and (*d*) delayed tumorigenesis in xenotransplantation models. Immunohistochemical analysis of tumor xenograft tissues following systemic treatment with saracatinib showed a reduction of tumor cell proliferation index, increased apoptosis, and diminished phospho-focal adhesion kinase and phospho-paxillin staining. Tumor stroma parameters such as angiogenesis or inflammatory infiltration were unaffected. In clonogenic survival assays, gastric carcinoma cells without addiction to Met were less sensitive than Met-addicted cells to Src inhibition.

**Conclusions**: Src is as a key downstream transducer of Met-driven tumor growth. Targeting Src might provide therapeutic benefit in Met-addicted tumors.

The Met tyrosine kinase receptor for hepatocyte growth factor is abnormally activated in a wide spectrum of human cancers because of gene amplification, transcriptional upregulation, point mutations, or ligand autocrine loops (1). Cell lines exhibiting amplification of the *MET* gene respond to Met inactivation with remarkable growth impairment, suggesting that this kind of genetic alteration drives "addiction" to Met activity*in vitro* and may predict effective treatment outcome *in vivo* (2, 3). These findings have spurred the development of several anti-Met antibodies and small-molecule Met inhibitors, many of which are now being tested in phase I and phase II clinical trials (1).

An emerging notion posits that therapeutic efficacy and treatment versatility could be improved by blockade of signals alternative to the main target and located either along the same pathway or in parallel pathways that synergize with respect to an essential function (4). In the case of Met, we reasoned that one such signal could be the Src tyrosine kinase. Met is a potent upstream activator of Src (5). During embryogenesis, Met-mediated activation of Src is necessary for trophoblast proliferation and proper placental formation, highlighting the contribution of Src to the execution of Met-dependent developmental fates related to tissue mass expansion (6); in cancer, dominant-negative isoforms of Src inhibit hepatocyte growth factor–induced growth of mammary carcinoma cells (7, 8) and impair the tumorigenic phenotype of NIH3T3 cells transformed by constitutively active mutants of Met (9). Moreover, Met and Src are often overexpressed (and coexpressed) in a vast number of human carcinomas (1, 10), and expression and activity of Met and Src can be comodulated (11); this suggests a functional collaboration between the two proteins and indicates that both kinases have not only epistatic but also cooperative roles in tumor progression.

Here we show that saracatinib, a small-molecule Src kinase inhibitor currently in phase II clinical trials (12, 13), displays a dose-dependent cytoreductive antitumor activity *in vitro*and *in vivo* in a panel of gastric carcinomas characterized by amplification of the *MET* gene and addicted to Met for growth and survival.

## MATERIALS AND METHODS

### Cell lines, compounds, antibodies, vectors, and viral infection

SNU5, HS746T, AGS, KATO III, and NCI-N87 were acquired from the American Type Culture Collection; MKN45 was purchased from Riken Cell Bank; GTL16 is a subclone of MKN45 obtained by limiting dilution (14). All cells were maintained in RPMI 1640 with 10% fetal bovine serum, 4 mmol/L glutamine, and antibiotics. The following antibodies were used: anti-human Met (Upstate Biotechnology); anti–phospho (Tyr1234/1235) Met, anti–phospho (Thr202/Tyr204) extracellular signal–regulated kinase (ERK), anti–phospho (Ser473) AKT, anti–cleaved caspase-3 (Cell Signaling); anti–phospho (Ty31349) Met, anti–phospho (Tyr861) focal adhesion kinase (FAK), anti–phospho (Tyr31) paxillin (BioSource International); anti-actin (Sigma); anti–Ki-67 (Dako); anti-CD31 (BD Biosciences); anti-CD45 (Abcam). PHA-665752 and dasatinib were purchased from Tocris Bioscience and Sequoia Research Products, respectively. For *in vivo* experiments, saracatinib was given as a suspension in 0.5% methylcellulose-0.2% Tween 80. Validated Mission shRNA lentiviral vectors targeting Src expression and control nontargeting shRNAs were purchased from Sigma-Aldrich. The Src shRNA sequences were as follows: for sh-Src1 (NM_198291.1-1579s1c1), CCGGGACAGACCTGTCCTTCAAGAACTCGAGTTCTTGAAGGA-CAGGTCTGTCTTTTTG; for sh-Src2 (NM_198291.1-1294s1c1), CCGGGTCATGAAGAAGCTGA-GGCATCTCAGATGCCTCAGCTTCTTCATGACTTTTTG. Viral vectors were produced by LipofectAMINE 2000 (Invitrogen)-mediated transient transfection of 293T. Infected cells were selected in medium with 100 ng/mL puromycin.

**Western blotting and densitometric analysis**

Proteins were extracted with boiling SDS buffer [50 mmol/L Tris-HCl (pH 7.5), 150 mmol/L NaCl, 1% SDS]. Extracts were clarified at 12,000 rpm for 15 minutes and normalized with the BCA Protein Assay Reagent Kit (Thermo Scientific). Proteins were electrophoresed on SDS-polyacrylamide gels and transferred onto nitrocellulose membranes (Hybond, Amersham). Nitrocellulose-bound antibodies were detected by the enhanced chemiluminescence system (Amersham). Blot images were captured using a ChemiDoc XRS molecular imager (Bio-Rad). Densitometric analysis was done with a Quantity One one-dimensional analysis software installed on the imager.

**cDNA microarrays and gene set enrichment analysis**

Total RNA was isolated with TRIzol (Invitrogen). For microarray analysis, reverse transcription and biotinylated cRNA synthesis were done using the Illumina TotalPrep RNA Amplification Kit (Ambion). Hybridization of the cRNAs was done on Sentrix HumanRef-8_v2 Expression BeadChips (24K, Illumina). Hybridized arrays were stained and scanned in a Beadstation 500 (Illumina). BeadStudio software (Illumina) was used to analyze raw data grouped by experimental condition. After rank-invariant normalization, genes were filtered for detection (>0.95 for all the experimental groups) and assessed for statistically significant differential expression using the Illumina custom test (iterative robust least squares fit). According to this test, a differential score higher than 30 corresponds to $P < 0.001$.

Gene set enrichment analysis (GSEA) was done using the publicly available desktop application from the Broad Institute (http://www.broad.mit.edu/gsea/software/software_index.html). Genes represented by more than one probe were collapsed using the XCollapseProbes utility to the probe with the maximum value. The gene set database used was that of curated sets, c2.v2.symbols.gmt. Due to the small number of samples, *P* values were calculated by permuting the genes 1,000 times. The classic enrichment statistic was selected.

**Soft-agar and cell viability assays**

Three thousand cells were resuspended in complete medium containing 0.5% Seaplaque agar. Cells were seeded in 24-well plates containing a 1% agar underlay and supplemented twice a week with complete medium in the presence or absence of saracatinib. Colonies were stained by incorporation of tetrazolium salts 2 weeks (for GTL16, MKN45, and KATO III) or 3 weeks (for HS746T, SNU5, AGS, and NCI-N87) after seeding. Colonies were coded and scored in a blinded fashion by a second observer. Colony numbers were obtained using a phase-contrast light microscope fitted with a 32-grid eyepiece at a total magnification of ×20. Images were captured with the ImageReady (Adobe) software using a microscope (Leica DMIL) and a 20× 0.30 objective (Leica) equipped with a digital camera (DFC320, Leica). For viability assays, 1,000 cells were resuspended in 50 μL of complete growth medium and seeded in 96-well plastic culture plates (day 0). On day 1, 50 μL of drugs or vehicle serially diluted in complete medium were added to cells. On day 4, cell viability was assessed by ATP content using a luminescence assay (CellTiter-Glo, Promega). All measurements were recorded using a DTX 880-Multimode plate reader (Beckman Coulter). Growth inhibition at each drug concentration was normalized to vehicle-treated cells.

**Tumorigenicity assays**

Cells ($2 \times 10^6$ for GTL16; $1 \times 10^6$ for MKN45; $3 \times 10^6$ for HS746T) were suspended in 200 μL of PBS and inoculated s.c. into the right posterior flank of 6-week-old immunodeficient*nu/nu* female mice on a Swiss CD1 background (Charles River Laboratories); tumors were measured every 2 or 3 days. Tumor volume was calculated with the formula $4/3\pi \times (d/2)^2 \times D/2$, where *d* is the minor

tumor axis and *D* is the major tumor axis. All animal procedures were approved by the Ethical Commission of the University of Torino, Italy, and by the Italian Ministry of Health.

**Tissue analysis and morphometry**

Xenograft tissues were fixed for 24 hours in 10% neutral buffered formalin and were then processed and paraffin embedded. Samples were cut into 5-μm-thick sections and immunostained with the appropriate antibodies. The VECTASTAIN ABC peroxidase/DAB staining kits (Vector) were used for immunohistochemical detection of Ki-67, cleaved caspase-3, phospho-paxillin, and phospho-FAK. Tissues were counterstained with hematoxylin, dehydrated, and mounted. Immunoreactivity for CD131 and CD145 was assessed by immunofluorescence using Alexa Fluor 488 or Alexa Fluor 546 (Invitrogen). Cell nuclei were labeled with 4′,6-diamidino-2-phenylindole (Invitrogen) and slides were mounted with Fluoromount-G (SouthernBiotech). Independent fields were quantified for every section (as indicated specifically for each experiment in the corresponding figure legend), and different sections of every tumor (as indicated in the figure legends) were analyzed using a Leica DM IRB microscope and quantified with the Metamorph software package (MDS Analytical Technologies).

**Statistics**

Results are mean ± SD for *in vitro* experiments and mean ± SEM for *in vivo* experiments. Comparisons were made using the two-tailed Student's *t* test. For dose-response cell viability assays and growth curves of xenografts, comparisons were made using two-way ANOVA. $P < 0.05$ was considered to be statistically significant.

## RESULTS AND DISCUSSION

**Src inhibition impairs anchorage-independent growth in a panel of Met-addicted gastric carcinoma cells**

GTL16, a gastric carcinoma cell line containing 11 extra copies of the *MET* locus (15), undergoes dramatic growth impairment in response to Met inhibition and is commonly considered a prototypic model to test drug sensitivity of Met-addicted tumors (2, 3, 16). We used the small-molecule Src kinase inhibitor saracatinib as a pharmacologic tool to block Src function. Saracatinib is a potent and selective inhibitor of Src and other Src tyrosine kinase family members and shows modest effects against Abl (10-fold less activity) and epidermal growth factor receptor (EGFR; 24-fold less activity). Saracatinib has been extensively characterized preclinically *in vitro* and *in vivo* (12, 13) and is now in phase II clinical trials.

Treatment of GTL16 with saracatinib did not affect proliferation in standard monolayer liquid culture in the presence of 10% serum (not shown); in contrast, saracatinib-mediated inhibition of Src potently impaired growth in soft agar, with a statistically significant effect observed at a concentration of 0.5 μmol/L and a complete inhibition plateau at 2 μmol/L (Fig. 1A). Formation of suspended colonies was inhibited both in absolute numbers (Fig. 1A, graph) and in size (Fig. 1A, images). To validate this result by alternative means, we inactivated Src using two other strategies: (*a*) dasatinib, a dual inhibitor of Src-family and Abl kinases (17); (*b*) short hairpin RNA (shRNA) interference, using two different shRNAs (sh-Src1 and sh-Src2). Similar to saracatinib, both dasatinib (Fig. 1A) and genetic silencing of Src (Fig. 1B) reduced GTL16 clonogenic growth in soft agar (with dasatinib exhibiting some weaker activity compared with saracatinib) without modifying the proliferation of adherent cells (not shown).

We also analyzed the effects of concomitant inhibition of Src and Met by quantitative viability assays in GTL16 cells cultured on plastic and treated with inhibitors against the two kinases for 72 hours. Under these conditions, tandem administration of a fixed amount of saracatinib (1 μmol/L) together with increasing concentrations of the Met-specific inhibitor PHA-665752 (16) resulted in a statistically significant left shift of the dose-response curve compared with administration of PHA-665752 alone ($P < 0.001$ by two-way ANOVA). For instance, inhibition of Met with 50 nmol/L PHA-665752 reduced cell viability by approximately 40%; at the same concentration of Met inhibitor, addition of saracatinib reduced viability by 67% (Fig. 1C). This indicates that inhibition of Src enhances cell sensitivity to inhibition of Met and lends support to the therapeutic potential of combinatorial treatments with Met and Src inhibitors.

To investigate whether Src inactivation is particularly effective in Met-addicted tumors, we expanded our soft-agar assays to additional gastric carcinoma cell lines exhibiting MET amplification and dependence on Met for continuous growth, as well as gastric carcinoma cells without MET amplification (2, 3). In MET-amplified MKN45 (from which GTL16 cells were clonally derived), HS746T, and SNU5, saracatinib-mediated inhibition of Src reduced anchorage-independent growth at compound doses similar to or even lower than those effective in GTL16 (Fig. 2A). In contrast, saracatinib was less active in Met-independent KATO III, AGS, and NCI-N87 gastric carcinoma cells, with statistically significant impairment of colony forming ability only at doses equal to or higher than 2 μmol/L (Fig. 2A). Congruent with this finding, Src pharmacologic inhibition by dasatinib or genetic inactivation by shRNA interference exerted little effects on the growth in soft agar of Met-independent KATO III cells (Fig. 2A and B) and no effects on their growth in monolayer culture (not shown). Thus, at least in the cellular models tested in this work, Met-dependent gastric carcinoma cells seem to be more sensitive than Met-independent cells to Src inactivation. However, it is noteworthy that saracatinib has been shown to inhibit the growth of other Met-independent cell lines of different tumor origins, including colon and prostate carcinomas (13). This indicates that the context of MET amplification/addiction, while correlating with cell sensitivity to Src inhibition, is not an absolute requirement for prediction of response to Src inhibitors.

**Signaling and transcriptional consequences of Src inhibition in Met-addicted gastric carcinoma cells**

We proceeded to investigate the biochemical and transcriptional consequences of Src inhibition in GTL16 cells. Given the technical difficulty in performing protein and mRNA extraction from colonies in soft agar, we decided to use cells cultured on plastic. Src deactivation does not affect the proliferation of GTL16 grown in monolayer; however, we assumed that detection of signaling and expression changes under this standard culture condition would disclose subthreshold priming events, which may become fully operative when cell viability is challenged by lack of anchorage.

The signaling effects of saracatinib were assessed using FAK, paxillin, AKT, and ERK1/2 as biomarkers of drug activity. FAK and paxillin are direct substrates of both Met and Src and amplify tyrosine kinase–dependent mitogenic and antiapoptotic signals through enzymatic (FAK) and scaffolding (FAK and paxillin) functions (18, 19). AKT and ERKs are conventional transducers of growth and survival signals (1, 19). Administration of saracatinib for 2 hours led to a dose-dependent reduction in the phosphorylation levels of FAK, paxillin, and AKT, but did not substantially affect the activation status of ERK1/2 (Fig. 3A). This is in consonance with recent reports indicating a preferential implication of Src in the activation of AKT rather than ERKs (20, 21).

Recently, a “reversed signal flow” whereby Met is passively transphosphorylated by Src family kinases has been reported in colon carcinoma cells (22, 23). To rule out that the effects of Src

inhibition are in fact mediated by dephosphorylation of Met, we treated GTL16 cells with suprasaturating concentrations of saracatinib for 1 hour and analyzed Met phosphotyrosine content. As shown in Fig. 3B, Src inhibition did not influence the overall tyrosine phosphorylation of Met in either the catalytic residues (Tyr1234 and Tyr1235) or Tyr1349 in the multifunctional docking site.

We further investigated the effect of Src inhibition by genome-wide expression profiling (24,000 genes interrogated). Consistent with the finding that Src inhibition is biologically neutral in adherent cells, treatment with 1 μmol/L saracatinib for 24 hours did not induce significant variations (fold change, >2; $P < 0.001$) in the expression of individual transcripts. Therefore, we decided to explore more subtle but functionally relevant modulations using the GSEA tool (24). This approach does not process transcripts as single entities. Rather, it considers gene sets (groups of genes related through a common function, pathway, or other property, according to published works) and tests whether the genes that are overexpressed or underexpressed in each profiled tissue or cell line include a higher-than-randomly-expected fraction of genes from a particular gene set. Among the gene sets significantly suppressed by saracatinib, there were signatures correlated with cell cycle progression, including transcripts induced by serum (SERUM_FIBROBLAST_CELLCYCLE), genes of the replication machinery (DNA_REPLICATION_REACTOME), genes involved in $G_1$-S progression (G1_TO_S_CELL_CYCLE_REACTOME), genes affected by Rb phosphorylation (VERNELL_PRB_CLSTR1), E2F1 targets (REN_E2F1_TARGETS), and genes downregulated by p21 and p53 (P21_ANY_DN and P21_P53_ANY_DN). Symmetrically, the transcripts repressed by serum stimulation were recovered among the saracatinib-induced gene sets (SERUM_FIBROBLAST_CORE_DN and CHANG_SERUM_RESPONSE_DN; Table 1). This transcriptional modulation is consistent with the impairment of anchorage-independent growth observed in response to Src inhibition.

**Inhibition of Src delays tumor growth in xenograft models of Met-addicted gastric carcinomas**

We extended the data obtained in the *in vitro* soft-agar assays to tumorigenesis *in vivo* by implanting subcutaneous xenografts of GTL16 cells in immunocompromised mice ($n = 10$ for each experimental condition). Following cell inoculation, animals were treated once daily with vehicle or increasing doses of saracatinib by oral gavage and tumor growth was monitored by caliper measurement. Continuous treatment for 1 month induced dose-dependent tumor responses, with a 29% end-point inhibition for a dose of 12.5 mg/kg/d and a 55% inhibition for doses of 25 and 50 mg/kg (Fig. 4). No visible toxic effects were observed. An analogous experiment was also done using GTL16 cells in which Src had been silenced by shRNA interference (Fig. 1B). Xenografts carrying sh-Src1 ($n = 6$) formed subcutaneous masses at slower rates than controls ($n = 6$), with a 44% reduction of tumor volume 1 month after injection (Fig. 4). Although manifest, inhibition of tumor growth following genetic depletion of Src was less pronounced than that achieved by saracatinib treatment, and differences did not reach statistical significance. This poorer effect might be caused by the emergence of polyclonal populations with incomplete suppression of Src due to variable numbers of integrated shRNA-expressing proviral vectors in individual cells; we suspect that cells with residual activity of Src were endowed with some growth advantage over cells with total Src abrogation and therefore underwent positive selection.

For confirmatory purposes, we repeated the xenotransplantation experiments using the other MET-amplified, Met-addicted gastric carcinoma cells already tested in the soft-agar assays. Similar to what was observed for GTL16 tumors, animals bearing xenografts of MKN45 ($n = 8$) and HS746T ($n = 6$) developed tumors with slower kinetics when dosed once daily with 50 mg/kg saracatinib; specifically, end-of-study tumor volumes were reduced by 56% in MKN45 and by 45% in HS746T

(Fig. 4). SNU5 cells were excluded because they proved to have a low frequency of subcutaneous engraftment and, in the (rare) cases of successful engraftment, displayed a very indolent growth (our unpublished observations).
In summary, systemic inhibition of Src retards the growth of Met-addicted gastric tumors *in vivo*. This is in contrast to the relatively inconsistent and modest tumor growth inhibition that has been reported for a range of xenograft tumor models (13) and may again reflect the close functional relationship between Src and Met.

**Inhibition of Src affects neoplastic growth by targeting the tumor cell compartment without perturbing the host microenvironment**

To investigate the mechanism by which Src inhibition negatively affects Met-dependent tumorigenesis, sections from end-of-study GTL16 xenografts were stained with antibodies to Ki-67 to assess the proportion of proliferating tumor cells and with antibodies to cleaved caspase-3 to assess the amount of apoptosis. As shown in Fig. 5A, Src-inhibited tumors displayed a 75% reduction of the proliferative index (Ki-67–positive cells) and a 3-fold increase of the apoptotic index (cleaved caspase-3–positive cells). These results suggest that blockade of Src signaling attenuates tumor growth *in vivo* by impairing both cell proliferation and cell survival. This is in agreement with the *in vitro* data on anchorage-independent growth, which is sustained by the acquired capability of cancer cells to both proliferate and resist apoptotic insults in the absence of matrix adhesion.

The consequences of systemic inactivation of Src on tumor growth could be due not only to direct effects on cancer cells but also to a subsidiary activity of the Src inhibitor in the microenvironment. Src activity is required for capillary formation (25) and regulation of vascular permeability (26). Hence, Src neutralization could mitigate two processes that commonly exacerbate the intrinsic malignant properties of neoplastic cells: intratumoral angiogenesis and, because of reduced blood cell extravasation, inflammatory stromal reaction. To address this issue, we decided to perform an *in situ* appraisal of various biological parameters: (*a*) tumor cell responses to Src inactivation were analyzed by evaluating the extent of Src-dependent intracellular signaling, using phospho-FAK and phospho-paxillin staining as molecular readouts; (*b*) host responses were analyzed by assessing tumor vascularization (using antibodies against the endothelial marker CD131) as well as stromal recruitment of inflammatory cells (using antibodies against the pan-leukocyte marker CD45).
We found that Src inhibition severely reduced the phosphorylation levels of both FAK and paxillin in tumor sections, indicating substantial deprivation of Src-dependent pathways in response to saracatinib treatment (Fig. 5B). This effect is analogous to that produced by other Src kinase inhibitors, such as dasatinib (27) and bosutinib (28). In contrast, host reactions were unaffected. We could not detect significant differences in vessel number and size between treated and untreated animals [vessels with diameter <10 μm per section: 32 ± 10 in untreated versus 28 ± 14 in saracatinib-treated ($P = 0.42$); vessels with diameter >10 μm per section: 23 ± 5 in untreated versus 22 ± 9 in saracatinib-treated ($P = 0.66$); $n = 14$; Fig. 5C]; similarly, the extent of inflammatory infiltration did not grossly change following saracatinib administration (Fig. 5C).
Collectively, these results indicate that systemic inhibition of Src impairs the growth of Met-addicted tumors by directly curtailing the proliferation and survival capabilities of tumor cells without influencing stromal functions. Lack of activity of saracatinib in the tumor microenvironment can be explained by the observation that Src-mediated modulation of angiogenesis and vascular permeability seems to be restricted to vascular endothelial growth factor–regulated processes; indeed, in $Src^{-/-}$ mice, vascular endothelial growth factor fails to regulate vessel sprouting and vascular permeability, whereas both activities properly occur in response to basic fibroblast growth

factor or inflammatory mediators (29). Because the tumor-reactive stroma contains many proangiogenic molecules and proinflammatory cytokines, it is conceivable that factors other than vascular endothelial growth factor can control tumor vascularization and vessel permeability in the presence of systemic Src blockade.

## CONCLUSIONS

It is now well established that the major determinant of responsiveness to targeted agents is the presence of a constitutively hyperactive form of the “druggable” oncoprotein, which arises from genetic corruptions such as point mutations, gene amplification, or chromosomal translocation. In the case of Met, oncogene addiction as a result of *MET*gene amplification may predict therapeutic response following Met inactivation (1–3). Therefore, treatment of MET-amplified, Met-addicted tumors with Met inhibitors should be considered the gold standard of care for such tumors. However, as suggested for other tyrosine kinase receptor–targeted therapies, the use of compounds that block Met-dependent signals is likely to prove valuable to increase efficacy, minimize systemic toxicities, and delay the emergence of drug resistance. Here, we provide evidence that Src tyrosine kinase is a crucial signaling effector of Met that, once inactivated, negatively affects Met-dependent tumorigenesis. Src neutralization alone seems to impair the growth of Met-addicted tumors, which suggests that Src inhibitors could be used sequentially to hold tumors in check during drug holidays from Met inhibitors. Moreover, because inhibition of Src enhances cell sensitivity to inhibition of Met (Fig. 1C), Src inhibitors could be combined with Met inhibitors to augment response and enable dose reduction compared with single-agent treatment.

Together with Src, other intracellular transducers known to convey Met-triggered tumorigenic signals include the Ras-RAF-MEK-ERK cascade and the phosphatidylinositol 3-kinase/AKT axis (30). RAF, MEK, and phosphatidylinositol 3-kinase inhibitors are now in clinical development (31, 32), and it is reasonable to argue that such inhibitors, similar to Src inhibitors, will be effective in limiting Met-driven oncogenesis. In patients, MET amplification is associated with both *de novo* and acquired resistance to the EGFR small-molecule inhibitor gefitinib in EGFR-mutant non–small-cell lung carcinomas (33–35). Interestingly, the extent of activation of Src is markedly increased in gefitinib-resistant non–small-cell lung carcinoma cells endowed with MET amplification compared with gefitinib-sensitive parental cells. Thus, Src inhibition may also attenuate the proliferative signals arising from crosstalk between Met and EGFR signaling (36), suggesting additional combined strategies to block tumor growth.

Our results provide a preclinical rationale and an experimental proof of concept for the use of compounds targeting Met downstream transducers as additional approaches to impair neoplastic progression in Met-dependent tumors.

### Disclosure of Potential Conflicts of Interest

P.M. Comoglio: commercial research grant and consultant/advisory board, AstraZeneca.


### Acknowledgments

We thank Antonello Galati for help with immunohistochemistry; Laura Tarditi, Tuti Werdiningsih, and Fabrizio Maina for animal care; Raffaella Albano, Stefania Giove, and Laura Palmas for technical assistance; and Antonella Cignetto for secretarial assistance.

**Grant Support**: AstraZeneca; Associazione Italiana per la Ricerca sul Cancro (E. Medico, P.M. Comoglio, and L. Trusolino); Compagnia di San Paolo and Fondazione Cassa di Risparmio di Torino (P.M. Comoglio); and Regione Piemonte (E. Medico, P.M. Comoglio, and L. Trusolino).

The costs of publication of this article were defrayed in part by the payment of page charges. This article must therefore be hereby marked *advertisement* in accordance with 18 U.S.C. Section 1734 solely to indicate this fact.

## REFERENCES

1. Comoglio PM, Giordano S, Trusolino L. Drug development of MET inhibitors: targeting oncogene addiction and expedience. Nat Rev Drug Discov 2008;7:504–16.
2. Smolen GA, Sordella R, Muir B, et al. Amplification of MET may identify a subset of cancers with extreme sensitivity to the selective tyrosine kinase inhibitor PHA-665752. Proc Natl Acad Sci U S A 2006;103:2316–21.
3. McDermott U, Sharma SV, Dowell L, et al. Identification of genotype-correlated sensitivity to selective kinase inhibitors by using high-throughput tumor cell line profiling. Proc Natl Acad Sci U S A 2007;104:19936–41.
4. Gossage L, Eisen T. Targeting multiple kinase pathways; a change in paradigm.Clin Cancer Res 2010;16:1973–8.
5. Mueller KL, Hunter LA, Ethier SP, Boerner JL. Met and c-Src cooperate to compensate for loss of epidermal growth factor receptor kinase activity in breast cancer cells. Cancer Res 2008;68:3314–22.
6. Maina F, Panté G, Heimbacher F, et al. Coupling Met to specific pathways results in distinct developmental outcomes. Mol Cell 2001;7:1293–306.
7. Rahimi N, Hung W, Tremblay E, Saulnier R, Elliott B. c-Src kinase activity is required for hepatocyte growth factor-induced motility and anchorage-independent growth of mammary carcinoma cells. J Biol Chem 1998;273:33714–21.
8. Bertotti A, Comoglio PM, Trusolino L. $\beta_4$-Integrin activates a Shp2-Src signaling pathway that sustains HGF-induced anchorage-independent growth. J Cell Biol2006;175:993–1003.
9. Nakaigawa N, Weirich G, Schmidt L, Zbar B. Tumorigenesis mediated by MET mutant M1268T is inhibited by dominant-negative Src. Oncogene2000;19:2996–3002.
10. Ishizawar R, Parsons SJ. c-Src and cooperating partners in human cancer. Cancer Cell 2004;6:209–14.
11. Cantiani L, Manara MC, Zucchini C, et al. Caveolin-1 reduces osteosarcoma metastases by inhibiting c-Src activity and met signaling. Cancer Res2007;67:7675–85.
12. Hennequin LF, Allen J, Breed J, et al. *N*- (5-Chloro-1,3-benzodioxol-4-yl)-7-[2-(4-methylpiperazin-1-y)ethoxy]-5-(tetrahydro-2*H*-pyran-4-yloxy)quinazolin-4-amine, a novel, highly selective orally available, dual-specific c-Src/Abl kinase inhibitor. J Med Chem 2006;49:6465–8.
13. Green TP, Fennell M, Whittaker R, et al. Preclinical anticancer activity of the potent, oral src inhibitor AZD0530. Mol Oncol 2009;3:248–61.
14. Giordano S, Di Renzo MF, Ferracini R, Chiadò-Piat L, Comoglio PM. p145, a protein with associated tyrosine kinase activity in a human gastric carcinoma cell line. Mol Cell Biol 1988;8:3510–7.
15. Rege-Cambrin G, Scaravaglio P, Carozzi F, et al. Karyotypic analysis of gastric carcinoma cell lines carrying an amplified c-met oncogene. Cancer Genet Cytogenet1992;64:170–3.
16. Christensen JG, Schreck R, Burrows J, et al. Mendel, a selective small molecule inhibitor of c-Met kinase inhibits c-Met-dependent phenotypes *in vitro* and exhibits cytoreductive antitumor activity *in vivo*. Cancer Res 2003;63:7345–55.
17. Lombardo LJ, Lee FY, Chen P, et al. Discovery of *N*-(2-chloro-6-methyl-phenyl)-2-(6(4-(2-hydroxyethyl)-piperazin-1-yl)-2-methylpyrimidin-4-ylamino)thiazole-5-carboxamide (BMS-354825),

a dual Src/Abl kinase inhibitor with potent antitumour activity in preclinical assays. J Med Chem 2004;47:6658–61.
18. Mitra SK, Schlaepfer DD. Integrin-regulated FAK-Src signaling in normal and cancer cells. Curr Opin Cell Biol 2006;18:516–23.
19. Ma PC, Tretiakova MS, Nallasura V, Jagadeeswaran R, Husain AN, Salgia R. Downstream signalling and specific inhibition of c-MET/HGF pathway in small cell lung cancer: implications for tumour invasion. Br J Cancer 2007;97:368–77.
20. Lu Y, Yu Q, Liu JH, et al. Src family protein-tyrosine kinases alter the function of PTEN to regulate phosphatidylinositol 3-kinase/AKT cascade. J Biol Chem2003;278:40057–66.
21. Chen Y, Guggisberg N, Jorda M, et al. Combined Src and aromatase inhibition impairs human breast cancer growth *in vivo* and bypass pathways are activated in AZD0530-resistant tumors. Clin Cancer Res 2009;15:3396–405.
22. Emaduddin M, Bicknell DC, Bodmer WF, Feller SM. Cell growth, global phosphotyrosine elevation, and c-Met phosphorylation through Src family kinases in colorectal cancer cells. Proc Natl Acad Sci U S A 2008;105:2358–62.
23. Leroy C, Fialin C, Sirvent A, et al. Quantitative phosphoproteomics reveals a cluster of tyrosine kinases that mediates SRC invasive activity in advanced colon carcinoma cells. Cancer Res 2009;69:2279–86.
24. Subramanian A, Tamayo P, Mootha VK, et al. Gene set enrichment analysis: a knowledge-based approach for interpreting genome-wide expression profiles. Proc Natl Acad Sci U S A 2005;102:15545–50.
25. Kilarski WW, Jura N, Gerwins P. Inactivation of Src family kinases inhibits angiogenesis *in vivo*: implications for a mechanism involving organization of the actin cytoskeleton. Exp Cell Res 2003;291:70–82.
26. Laird AD, Li G, Moss KG, et al. Src family kinase activity is required for signal tranducer and activator of transcription 3 and focal adhesion kinase phosphorylation and vascular endothelial growth factor signaling *in vivo* and for anchorage-dependent and -independent growth of human tumor cells. Mol Cancer Ther 2003;2:461–9.
27. Serrels A, Macpherson IRJ, Evans TRJ, et al. Identification of potential biomarkers for measuring inhibition of src kinase activity in colon cancer cells following treatment with dasatinib. Mol Cancer Ther 2006;5:3014–22.
28. Golas JM, Lucas J, Etienne C, et al. SKI-606, a Src/Abl inhibitor with *in vivo* activity in colon tumour xenograft models. Cancer Res 2005;65:5358–64.
29. Eliceiri BP, Paul R, Schwartzberg PL, Hood JD, Leng J, Cheresh DA. Selective requirement for Src kinases during VEGF-induced angiogenesis and vascular permeability. Mol Cell 1999;4:915–24.
30. Bertotti A, Burbridge MF, Gastaldi S, et al. Only a subset of Met-activated pathways are required to sustain oncogene addiction. Sci Signal 2009;2:ra80.
31. Engelman JA, Chen L, Tan X, et al. Effective use of PI3K and MEK inhibitors to treat mutant Kras G12D and PIK3CA H1047R murine lung cancers. Nat Med2008;14:1351–6.
32. Wong KK. Recent developments in anticancer agents targeting the Ras/Raf/MEK/ERK pathway. Recent Pat Anticancer Drug Discov 2009;4:28–35.
33. Bean J, Brennan C, Shih JY, et al. MET amplification occurs with or without T790M mutations in EGFR mutant lung tumors with acquired resistance to gefitinib or erlotinib. Proc Natl Acad Sci U S A 2007;104:20932–7.
34. Engelman JA, Zejnullahu K, Mitsudomi T, et al. MET amplification leads to gefitinib resistance in lung cancer by activating ERBB3 signaling. Science 2007;316:1039–43.
35. Sequist LV, Martins RG, Spigel D, et al. First-line gefitinib in patients with advanced non-small-cell lung cancer harboring somatic EGFR mutations. J Clin Oncol 2008;26:2442–9.

36. Yoshida T, Okamoto I, Okamoto W, et al. Effects of src inhibitors on cell growth and epidermal growth factor receptor and Met signaling in gefitinib-resistant non-small cell lung cancer cells with acquired Met amplification. Cancer Sci 2010;101:167–72

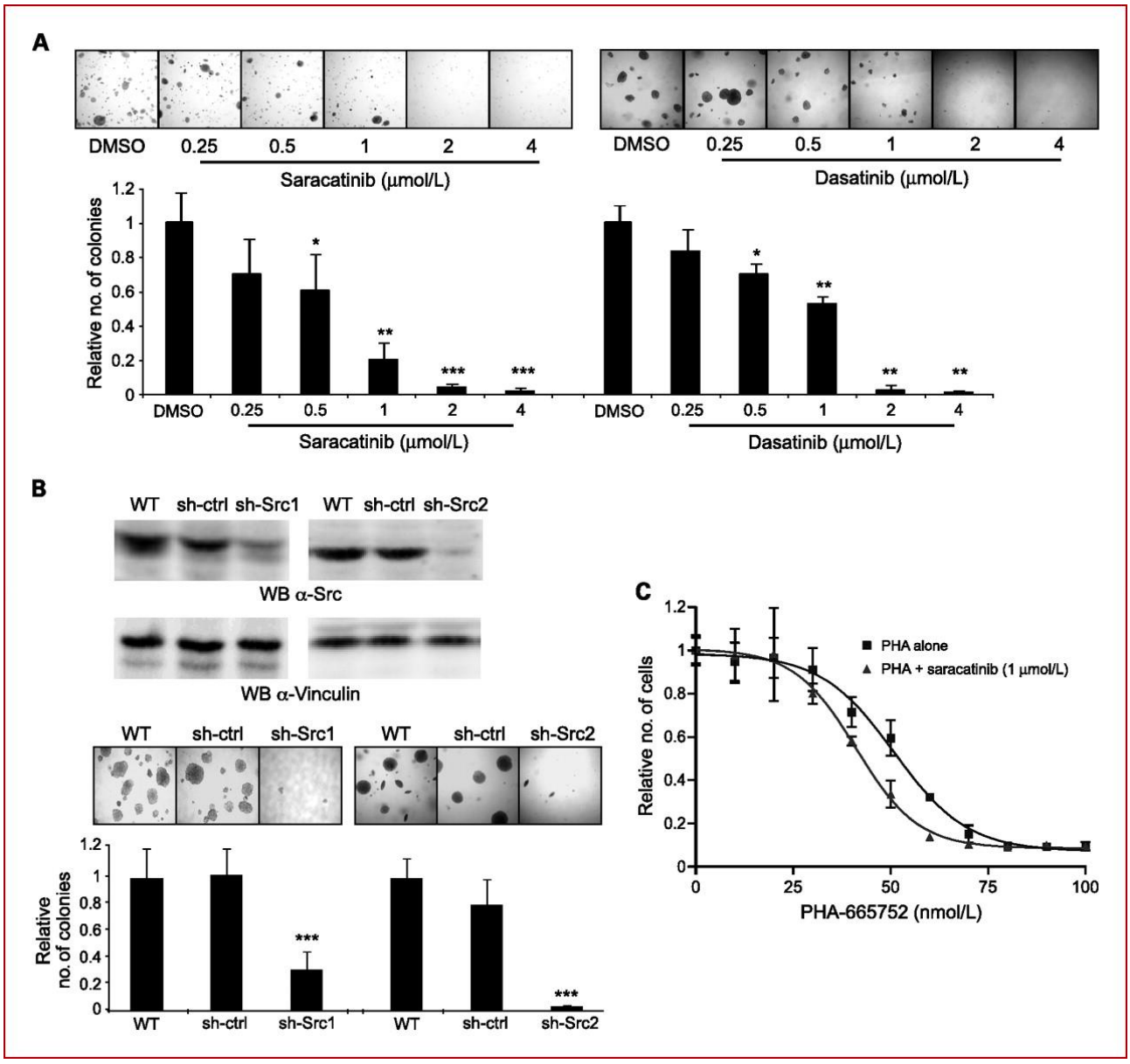


**Fig. 1.**

Src inhibition impairs anchorage-independent growth of Met-addicted gastric carcinoma cells and enhances sensitivity to Met inhibition. A, representative images and quantitation of soft-agar assays in GTL16 cells treated with the indicated concentrations of saracatinib or dasatinib. B, shRNA-mediated knockdown of Src (top) inhibits growth in soft agar (bottom). WT, wild-type GTL16 cells; sh-ctrl, cells infected with a nontargeting shRNA; sh-Src1 and sh-Src2, cells infected with two different Src-specific shRNAs. C, growth inhibition of GTL16 cells treated with increasing concentrations of the Met inhibitor PHA-665752 (PHA), alone or in combination with 1 μmol/L saracatinib. Columns, mean of two independent experiments done in quadruplicate; bars, SD. *, $P < 0.05$; **, $P < 0.01$; ***, $P < 0.001$.

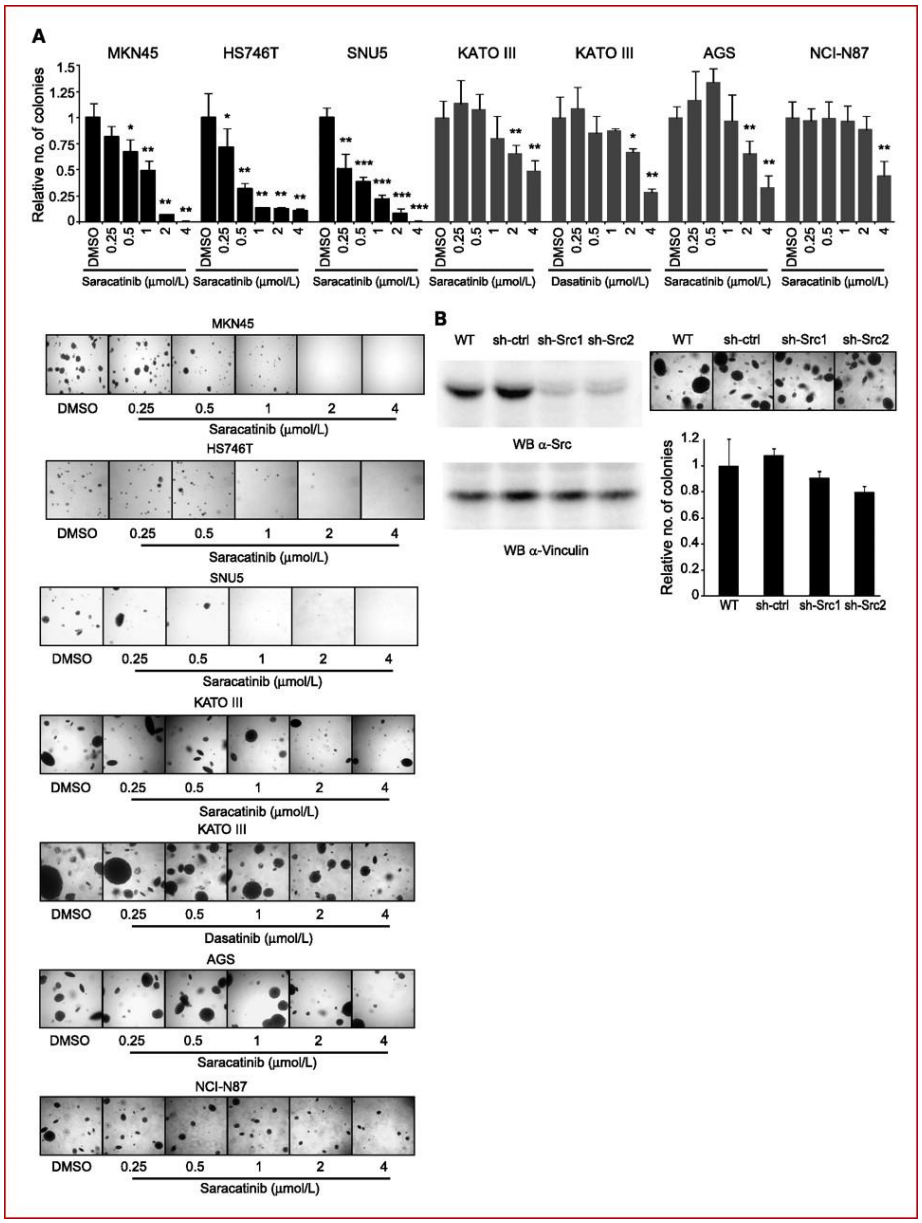


**Fig. 2.**

Src inhibition impairs growth in soft agar more efficiently in Met-dependent than in Met-independent gastric carcinoma cells. A, quantitation and representative images of soft-agar assays in the indicated cell lines, in the presence or absence of saracatinib or dasatinib. Black histograms, Met-addicted cell lines; gray histograms, Met-independent cell lines. B, in KATO III cells, shRNA-mediated knockdown of Src (left) exerts negligible effects on growth in soft agar (right). Columns, means of two independent experiments done in quadruplicate; bars, SD. *, $P < 0.05$; **, $P < 0.01$; ***, $P < 0.001$.

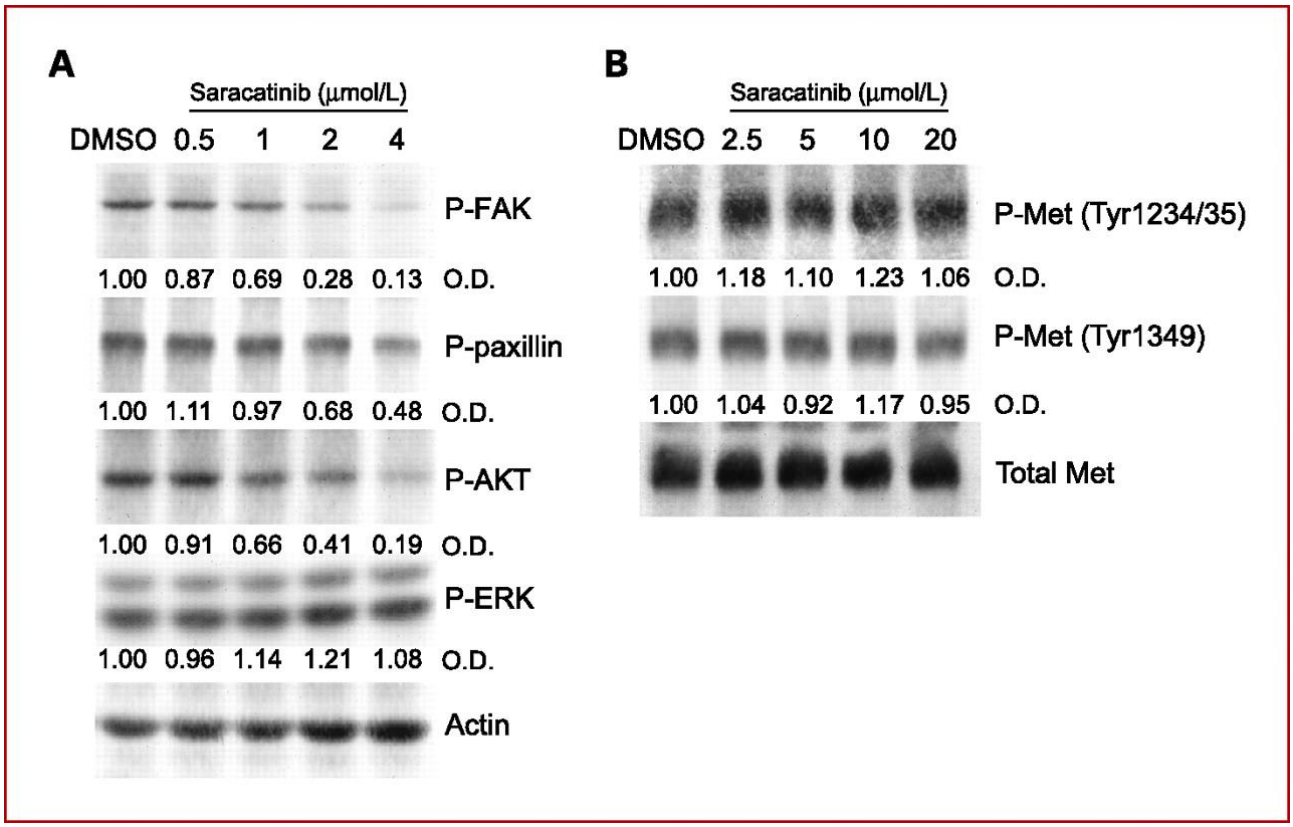


**Fig. 3.**

Signaling consequences of Src inhibition in GTL16 cells. A, dose-response curves of FAK, paxillin, AKT, and ERK1/2 phosphorylation in GTL16 cells treated with increasing concentrations of saracatinib. Actin was used as a loading control. Protein phosphorylation was quantitated by densitometric analysis (O.D.) relative to actin. B, Met phosphorylation is not impaired by suprasaturating doses of saracatinib. Met phosphorylation was quantitated by densitometric analysis (O.D.) relative to Met total protein.

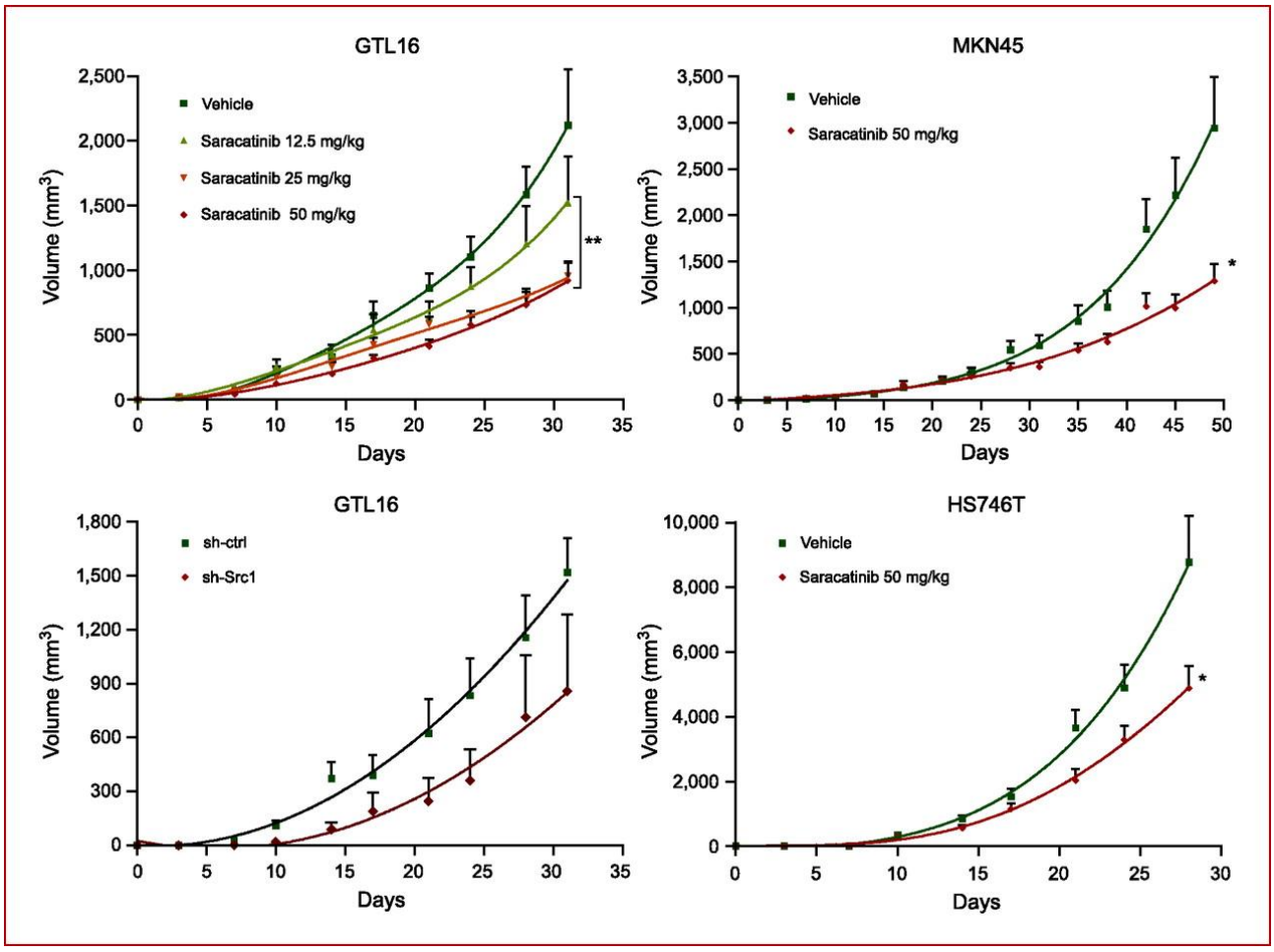


**Fig. 4.**

Inhibition of Src delays tumor growth in xenografts of Met-addicted gastric carcinomas. Growth curves of xenografts from wild-type GTL16, GTL16 infected with a nontargeting shRNA (sh-ctrl) or with a Src-specific shRNA (sh-Src1), MKN45, and HS746T gastric carcinoma cells in nude mice. *, $P < 0.05$; **, $P < 0.01$. Points, mean; bars, SEM.

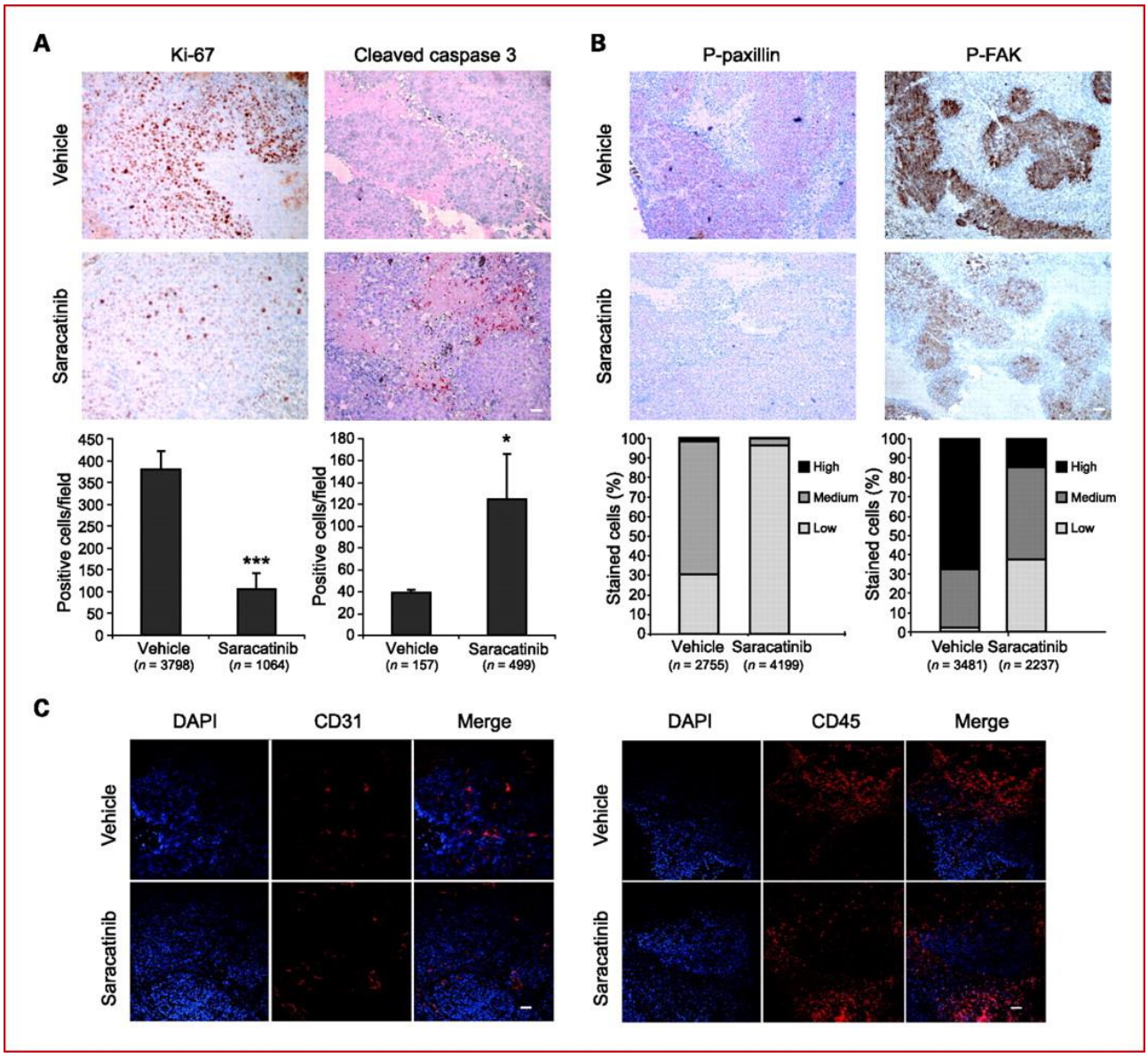


**Fig. 5.**

Systemic inhibition of Src affects the growth of GTL16 xenografts by tumor-autonomous mechanisms. For the quantitations shown in this figure, six tumors per each experimental group (vehicle or saracatinib treated) were analyzed; for each tumor, at least three sections and 10 fields were counted. Bar, 50 μm. A, proliferation index (Ki-67) and apoptotic index (cleaved caspase-3). B, phospho-paxillin and phospho-FAK staining. C, tumor vascularization (CD31, red) and leukocyte infiltration (CD45, red). Nuclei were marked with 4′,6-diamidino-2-phenylindole (DAPI; blue). *, $P < 0.05$; ***, $P < 0.001$. Columns, mean; bars, SD.

**Table 1.**

GSEA analysis of the transcriptional response produced by Src pharmacologic inhibition in GTL16 cells

| Rank | Gene set | Size | ES | NES | NOM *P* | FDR *q* | Expression |
|---|---|---|---|---|---|---|---|
| 1 | REN_E2F1_TARGETS | 39 | −0.69 | −2.48 | <0.0001 | <0.0001 | Down |
| 2 | DNA_REPLICATION_REACTOME | 43 | −0.68 | −2.47 | <0.0001 | <0.0001 | Down |
| 3 | SERUM_FIBROBLAST_CELLCYCLE | 113 | −0.57 | −2.45 | <0.0001 | <0.0001 | Down |
| 4 | VERNELL_PRB_CLSTR1 | 56 | −0.63 | −2.41 | <0.0001 | <0.0001 | Down |
| 8 | P21_ANY_DN | 28 | −0.71 | −2.3 | <0.0001 | 0 | Down |
| 16 | P21_P53_ANY_DN | 43 | −0.57 | −2.04 | <0.0001 | 0.01 | Down |
| 17 | G1_TO_S_CELL_CYCLE_REACTOME | 59 | −0.53 | −2.03 | 0 | 0.01 | Down |
| 4 | CHANG_SERUM_RESPONSE_DN | 97 | 0.66 | 2.61 | <0.0001 | <0.0001 | Up |
| 5 | SERUM_FIBROBLAST_CORE_DN | 153 | 0.6 | 2.53 | <0.0001 | <0.0001 | Up |

NOTE: The gene sets, all statistically significant, have been selected based on their functional importance.

Abbreviations: ES, enrichment score; NES, normalized enrichment score; NOM, nominal; FDR, false discovery rate.